

ON THE FORMATION OF GLYCOLALDEHYDE IN DENSE MOLECULAR CORES

PAUL M. WOODS¹, GEORGE KELLY¹, SERENA VITI¹, BEN SLATER², WENDY A. BROWN², FABRIZIO PULETTI²,
DAREN J. BURKE², AND ZAMAAN RAZA²

¹ Department of Physics and Astronomy, University College London, Gower Street, London WC1E 6BT, UK; paul.woods@ucl.ac.uk

² Department of Chemistry, University College London, 20 Gordon Street, London WC1H 0AJ, UK

Received 2011 November 21; accepted 2012 February 22; published 2012 April 11

ABSTRACT

Glycolaldehyde is a simple monosaccharide sugar linked to prebiotic chemistry. Recently, it was detected in a molecular core in the star-forming region G31.41+0.31 at a reasonably high abundance. We investigate the formation of glycolaldehyde at 10 K to determine whether it can form efficiently under typical dense core conditions. Using an astrochemical model, we test five different reaction mechanisms that have been proposed in the astrophysical literature, finding that a gas-phase formation route is unlikely. Of the grain-surface formation routes, only two are efficient enough at very low temperatures to produce sufficient glycolaldehyde to match the observational estimates, with the mechanism culminating in $\text{CH}_3\text{OH} + \text{HCO}$ being favored. However, when we consider the feasibility of these mechanisms from a reaction chemistry perspective, the second grain-surface route looks more promising, $\text{H}_3\text{CO} + \text{HCO}$.

Key words: astrochemistry – ISM: abundances – ISM: clouds – ISM: molecules – stars: formation

Online-only material: color figure

1. INTRODUCTION

The chemistry of dense molecular cores—the birth sites of massive stars—is demonstrably complex, in that large molecules composed of several functional groups are observed to be present. Of particular interest for their astrobiological implications (Remijan et al. 2004; Snyder 2006) are the isomers of composition $\text{C}_2\text{H}_4\text{O}_2$, viz. methyl formate, acetic acid, and glycolaldehyde. Glycolaldehyde (CH_2OHCHO), a simple monosaccharide sugar linked with the formation of RNA and amino acids in terrestrial environments (Collins & Ferrier 1995; Weber 1998), was detected first toward the Galactic center molecular cloud Sagittarius B2(N) (Hollis et al. 2000), and more recently toward a star-forming hot molecular core, G31.41+0.31 (Beltrán et al. 2009), both rich sources of molecules.

The mechanism of glycolaldehyde formation in these environments is uncertain, although it is becoming increasingly clear that the site of the formation of large organic molecules is the icy surfaces of astronomical dust (e.g., Garrod et al. 2006). As suggested by early models of grain-surface chemistry, much of the development of complex molecules is through fairly rapid hydrogenation of frozen out gas-phase molecules (e.g., Tielens & Whittet 1997). Once the end points of these processes have been reached (e.g., $\text{C} \rightarrow \text{CH}_3\text{OH}$, $\text{N} \rightarrow \text{NH}_3$), molecules and radicals must move through the ice structures in order to build the large organic molecules we detect in regions of star formation.

In this paper, we investigate the formation of glycolaldehyde in a collapsing cloud core at 10 K by comparing five mechanisms that have been suggested in the astrophysical literature. These mechanisms are highly speculative; all are without associated reaction rate coefficients and many of the reactions involved have not previously been included in astrochemical models to assess their effectiveness. We aim to constrain the possible formation routes of glycolaldehyde in cold cores, by investigating the wide parameter space resulting from the lack of existing constraints. This work is an initial investigation which forms part of a larger program looking into the formation of glycolaldehyde

in the dense interstellar medium, using the combined tools of astrochemical modeling, experimental surface chemistry, and quantum chemical calculations.

Dense prestellar cores have a very limited range of temperatures, from ~ 7 –11 K (e.g., Pagani et al. 2007; Bergin et al. 2006; Lai et al. 2003; Hotzel et al. 2002), and there is experimental evidence (Öberg et al. 2009; Bennett & Kaiser 2007b) that glycolaldehyde forms in such low-temperature environments. Given the uncertainties in reaction rates, we look at a large parameter space, and conservatively restrict ourselves to simple hydrogenation of the species which are frozen out onto grain surfaces. In this way, we identify which of the mechanisms suggested in an ad hoc manner are feasible for the production of glycolaldehyde in molecular cores such as G31.41+0.31. In Section 2, we give details on the selected mechanisms which we investigate. Section 3 gives an overview of our model, and the procedure which we follow in investigating the mechanisms. In Sections 4 and 5, we draw out some results from our modeling, and evaluate them bearing the chemical energetics of the reactions in mind. In Section 6, we conclude with a summary of our findings.

2. PROPOSED PATHWAYS TO GLYCOLALDEHYDE

Since its detection in space, there has been significant interest in glycolaldehyde formation (e.g., Sorrell 2001; Charnley & Rodgers 2005; Halfen et al. 2006; Bennett & Kaiser 2007b; Beltrán et al. 2009, and others). Several mechanisms for this have been proposed, including both gas-phase and surface reactions, and experiments have been conducted on laboratory surface analogs. We summarize some of the work which has been carried out below, and in Table 1. We do not consider high-temperature (~ 300 K) formation routes, e.g., Jalbout et al. (2007).

Some of these reactions have been tested in hot core models, at temperatures up to 200 K. For example, Garrod et al. (2008; and, presumably, Laas et al. 2011) incorporate reactions B3 and E6. However, the chemistry in these warm temperature regimes

Table 1
Summary of Proposed Reaction Pathways

Reaction	Reference	Medium	Method
A1. $g\text{-H}_2\text{O} + h\nu \rightarrow g\text{-OH} + g\text{-H}$ A2. $g\text{-CH}_4 + h\nu \rightarrow g\text{-CH}_3 + g\text{-H}$ A3. $g\text{-CH}_3 + g\text{-OH} \rightarrow g\text{-CH}_3\text{OH}$ A4. $g\text{-CO} + g\text{-H} \rightarrow g\text{-HCO}$ A5. $g\text{-CH}_3\text{OH} + g\text{-HCO} \rightarrow g\text{-CH}_2\text{OHCHO} + g\text{-H}$	Sorrell (2001)	Grain mantle ($\text{H}_2\text{O}/\text{CH}_4/\text{NH}_3/\text{CO}$)	Theory
B1. $g\text{-CH}_3\text{OH} + \text{CRP} \rightarrow g\text{-CH}_2\text{OH} + g\text{-H}$ B2. $g\text{-CO} + g\text{-H} \rightarrow g\text{-HCO}$ B3. $g\text{-CH}_2\text{OH} + g\text{-HCO} \rightarrow g\text{-CH}_2\text{OHCHO}$	Bennett & Kaiser (2007b)	Grain mantle ($\text{CH}_3\text{OH}/\text{CO}$)	Experiment
C1. $\text{H}_3^+ + \text{H}_2\text{CO} \rightarrow \text{H}_2\text{COH}^+ + \text{H}_2$ C2. $\text{H}_2\text{COH}^+ + \text{H}_2\text{CO} \rightarrow \text{CH}_2\text{OHCH}_2\text{O}^+$ C3. $\text{CH}_2\text{OHCH}_2\text{O}^+ \rightarrow \text{CH}_2\text{OHCHOH}^+$ C4. $\text{CH}_2\text{OHCHOH}^+ \rightarrow \text{CH}_2\text{OHCHO} + \text{H}^+$	Halfen et al. (2006)	Gas	Theory
D1. $g\text{-CO} + g\text{-H} + g\text{-H} \rightarrow g\text{-H}_2\text{CO}$ D2. $g\text{-CO} + g\text{-H} \rightarrow g\text{-HCO}$ D3. $g\text{-H}_2\text{CO} + g\text{-HCO} + g\text{-H} \rightarrow g\text{-CH}_2\text{OHCHO}$	Beltrán et al. (2009)	Surface	Theory
E1. $g\text{-CO} + g\text{-H} \rightarrow g\text{-HCO}$ E2. $g\text{-HCO} + g\text{-C} \rightarrow g\text{-HC}_2\text{O}$ E3. $g\text{-HC}_2\text{O} + g\text{-H} \rightarrow g\text{-CH}_2\text{CO}$ E4. $g\text{-CH}_2\text{CO} + g\text{-H} \rightarrow g\text{-CH}_2\text{CHO}$ E5. $g\text{-CH}_2\text{CHO} + g\text{-O} \rightarrow g\text{-OCH}_2\text{CHO}$ E6. $g\text{-OCH}_2\text{CO} + g\text{-H} \rightarrow g\text{-CH}_2\text{OHCHO}$	Charnley & Rodgers (2005)	Surface	Theory

Note. g - signifies a grain-surface species, $h\nu$ signifies a UV photon, and CRP signifies a cosmic-ray particle.

is somewhat different, since surface radicals can be sufficiently energetic to overcome diffusion barriers, affording them greater mobility on grain surfaces. We only consider these reactions at 10 K in order to test whether glycolaldehyde can form efficiently in the isothermal collapse phase of star formation.

Below, we summarize the work from which the reaction mechanisms in Table 1 comes.

2.1. Mechanism A

Sorrell (2001) discusses the theory of processing icy grain mantles in the interstellar medium with ultraviolet (UV) radiation, producing high concentrations of free radicals (particularly OH and CH₃). These radicals then react in the grain mantles in order to produce large organic molecules such as amino acids and sugars, with the energy for thermal hopping coming from grain–grain collisions. The resulting large organics (including glycolaldehyde) would then be desorbed into the gas phase following mantle explosions, and despite some fraction of these large molecules being destroyed in the process, some would remain intact.

2.2. Mechanism B

Bennett & Kaiser (2007b) simulated the bombardment of grain mantles with cosmic-ray particles by irradiating laboratory methanol/carbon monoxide ices with energetic electrons at 11 K. Cosmic rays can penetrate entire grains, producing up to 100 suprathreshold particles each, which then ionize (methane) ice molecules (Kaiser et al. 1997; Kaiser 2002). The resulting high-energy electrons (~5 keV) may then affect the mantle chemistry by forming radicals, which subsequently react to form large organic molecules. In a methanol/carbon monoxide ice these large organics include C₂H₄O₂ isomers. The experiment showed that both glycolaldehyde and methyl formate were formed, in addition to many smaller molecules and radicals. Acetic acid was not detected, but can be formed in methane/carbon dioxide ices (Bennett & Kaiser 2007a).

2.3. Mechanism C

Halfen et al. (2006) postulate that glycolaldehyde may be formed in the gas phase through acid-catalyzed reactions of formaldehyde, based on research on formose reactions (Butlerow 1861; Breslow 1959). Formaldehyde would react with its protonated form to create an intermediate species, which would then undergo reorganization into protonated glycolaldehyde. There is some experimental evidence for this method, although it is unclear whether the resulting C₂H₄O₂ isomer is in fact glycolaldehyde (Jalbout et al. 2007).

2.4. Mechanism D

Beltrán et al. (2009) highlighted the potential importance of the HCO radical in glycolaldehyde formation. They suggested that reactions between HCO and methanol (or methanol derivatives) or formaldehyde could occur rapidly on grain surfaces in hot cores. Gas-phase routes would be too inefficient. The simplicity of the reaction pathway, which is driven by rapid hydrogenation and the reaction of small surface radicals, means that glycolaldehyde formation could be efficient when densities are high. Only small amounts of CO would need to be processed on grains.

2.5. Mechanism E

Charnley & Rodgers (2005) suggested that complex molecules build up on grain surfaces through the aggregation of common atoms, since at low temperatures only atoms are likely to be mobile. At early times, atoms such as C, N, or O may accrete significantly, whereas at late times, when most heavy atoms will have frozen out, hydrogenation of molecules will dominate. Such a scheme could not only lead to the formation of glycolaldehyde, but also to other large molecules such as acetic acid and aminomethanol. Methyl formate, however, cannot be formed through this kind of pathway, but only through the combination of relatively large surface radicals.

Table 2
Hydrogenation Percentages for Accreting Species

Accreting Species	Products in Regime 1 (f1)	Products in Regime 2 (f2)
O	2% O, 18% OH, 80% H ₂ O	1% O, 9% OH, 90% H ₂ O
CO	70% CO, 20% HCO, 5% H ₂ CO, 5% CH ₃ OH	60% CO, 25% HCO, 10% H ₂ CO, 5% CH ₃ OH
C	2% C, 3% CH, 5% CH ₂ , 20% CH ₃ , 70% CH ₄	1% C, 4% CH, 8% CH ₂ , 12% CH ₃ , 75% CH ₄
HCO ⁽⁺⁾	20% HCO, 40% H ₂ CO, 40% CH ₃ OH	10% HCO, 45% H ₂ CO, 45% CH ₃ OH
OH	10% OH, 90% H ₂ O	5% OH, 95% H ₂ O

3. THE CHEMICAL MODEL AND SCIENTIFIC PROCEDURE

In order to test which of the suggested routes to glycolaldehyde formation are feasible in dense core environments, we have incorporated the above chemical reactions (Table 1) into a model of a hot molecular core. The model, described below in more detail, is based on that described in Viti et al. (2004).

3.1. The Model

The model is a two-phase time-dependent model which follows the collapse of a prestellar core (phase I), followed by the subsequent warming and evaporation of grain mantles (phase II). We only consider phase I, since in this work we wish to investigate the potential formation of glycolaldehyde at low temperatures, as suggested by experiment (Öberg et al. 2009; Bennett & Kaiser 2007b). In phase I, a diffuse cloud of density 10^2 molecules cm^{-3} undergoes free-fall collapse until it has reached a density of $\sim 10^7$ cm^{-3} . This occurs on a timescale of half a million years and at a temperature of 10 K. During the collapse, atoms and molecules collide with, and freeze on to, grain surfaces. We assume that hydrogenation occurs rapidly on these surfaces, so that, for example, some percentage of carbon atoms accreting will rapidly become frozen out methane, CH₄. Initial atomic abundances are taken from Sofia & Meyer (2001), as in Viti et al. (2004). We employ the reaction rate data from the UDfA06³ astrochemical database, augmenting it with grain-surface (hydrogenation) reactions and those reactions included in Table 1. In the formation of glycolaldehyde we only consider the most propitious of circumstances. We discount the destruction of glycolaldehyde on the grains through cosmic ray strikes, photodissociation or further reaction, so that the quantity of glycolaldehyde formed can be regarded as an upper limit. We also assume that, due to the cold temperature, no species will desorb from the grains except H and He. This assumption is reasonable when considering thermal desorption, but neglects the effect of non-thermal desorption mechanisms on both glycolaldehyde and the reactants which go into its formation. Any proposed reaction pathways that do not produce reasonable amounts of glycolaldehyde under these conditions can surely be dismissed from consideration.

3.2. The Procedure

First, we investigate the five schemes individually, varying key model parameters, such as the rate coefficients, the final collapse density, the incident UV field, the cosmic-ray ionization rate, and the hydrogenation efficiency of accreted molecules. Finally, we look at all the mechanisms together, to find which is the most efficient in competition.

Many of the rate coefficients of the reactions in Table 1 are completely unknown. In light of this, we consider a wide parameter space, covering up to 14 orders of magnitude in reaction rate. Our aim is to understand the behavior of the reactions in each mechanism, and what effect they have on the abundance of glycolaldehyde, not to determine reaction rates. However, through our investigation we may be able to better constrain possible reaction rates. Where practical, we adopt identical or similar gas-phase reaction rates from UDfA06 or KIDA⁴ for unknown grain-surface rates as a conservative initial estimate (Table 3), given that the grain surface is thought to act as a catalyst. Glycolaldehyde is not included in the standard UDfA06 database, so we utilize rates from analogous reactions which produce methyl formate, or we make very conservative estimates. In varying the rates, we vary only the α -parameter in the rate coefficients: $k = \alpha(T/300\text{ K})^\beta \exp(-\gamma/T)$ for two-body reactions, $k = \alpha$ for reactions with cosmic rays, and $k = \alpha \exp(-\gamma A_V)$ for photoreactions.

We test two final collapse densities, $n_f = 10^6$ and 10^7 cm^{-3} , which also have implications for the freezeout percentage of molecules. Viti et al. (2001) argued that in hot cores freezeout is never total and in fact some gaseous CO is always observed, even in regions where no millimeter continuum is detected (e.g., Molinari et al. 2000). Hence, we impose the constraint that a maximum of 90% of the circumstellar material is frozen out at a final density of $n_f = 10^7$ cm^{-3} , and 75% at 10^6 cm^{-3} .

The strength of the impinging UV field within the core was adjusted solely for mechanism A, since it involves the UV processing of molecules on grains. We investigated the effects of scaling the standard interstellar UV field strength, G_0 , by up to 30 times. When investigating reaction B1, we increase the cosmic-ray ionization rate in the model globally by up to 1000 times.

Finally, we tested two different grain-surface hydrogenation regimes, one where the products were more saturated (“f2”) and one less saturated (“f1”). These regimes are represented in Table 2. Hydrogenation rates on grain surfaces are unknown, but the calculation of hydrogen-atom hopping and tunneling rates shows that they are rapid in comparison to other grain-surface reactions (Goumans et al. 2007; Tielens 1989). At low temperatures, the recombination of physisorbed atomic hydrogen with chemisorbed atoms dominates. At temperatures < 20 K, molecular hydrogen formation efficiency on grain surfaces is near unity (Cazaux & Tielens 2004; Williams et al. 2007). We assume that hydrogenation of species on grain surfaces is instantaneous.

We combine these free parameters into a grid of model results.

4. RESULTS

We have calculated approximately 450 models to investigate the formation of glycolaldehyde at 10 K during the isothermal collapse phase of star formation. Many of these permutations

³ <http://www.udfa.net>

⁴ <http://kida.obs.u-bordeaux1.fr>

Table 3
Adopted Reaction Rates for Key Reactions

Reaction	α Coefficient	Comment
A1. $g\text{-H}_2\text{O} + h\nu \rightarrow g\text{-OH} + g\text{-H}$	5.9×10^{-10} ($\gamma = 1.7$)	Based on gas phase
A2. $g\text{-CH}_4 + h\nu \rightarrow g\text{-CH}_3 + g\text{-H}$	2.2×10^{-10} ($\gamma = 2.2$)	Based on gas phase
A3. $g\text{-CH}_3 + g\text{-OH} \rightarrow g\text{-CH}_3\text{OH}$	1.0×10^{-9}	Based on similar gas phase
A4. $g\text{-CO} + g\text{-H} \rightarrow g\text{-HCO}$...	Assumed fast
A5. $g\text{-CH}_3\text{OH} + g\text{-HCO} \rightarrow g\text{-CH}_2\text{OHCHO} + g\text{-H}$	3.0×10^{-17}	Methyl formate rate retarded by $\times 50$
B1. $g\text{-CH}_3\text{OH} + \text{CRP} \rightarrow g\text{-CH}_2\text{OH} + g\text{-H}$	1.3×10^{-17}	Standard ζ (CRP = cosmic ray)
B2. $g\text{-CO} + g\text{-H} \rightarrow g\text{-HCO}$...	Assumed fast
B3. $g\text{-CH}_2\text{OH} + g\text{-HCO} \rightarrow g\text{-CH}_2\text{OHCHO}$	3.0×10^{-17}	Conservative estimate
C1. $\text{H}_3^+ + \text{H}_2\text{CO} \rightarrow \text{H}_2\text{COH}^+ + \text{H}_2$	6.3×10^{-9}	Based on similar gas phase
C2. $\text{H}_2\text{COH}^+ + \text{H}_2\text{CO} \rightarrow \text{CH}_2\text{OHCH}_2\text{O}^+$	1.0×10^{-10}	Based on similar gas phase
C3. $\text{CH}_2\text{OHCH}_2\text{O}^+ \rightarrow \text{CH}_2\text{OHCHOH}^+$...	Assumed fast
C4. $\text{CH}_2\text{OHCHOH}^+ \rightarrow \text{CH}_2\text{OHCHO} + \text{H}^+$...	Assumed fast
D1. $g\text{-CO} + g\text{-H} + g\text{-H} \rightarrow g\text{-H}_2\text{CO}$...	Assumed fast
D2. $g\text{-CO} + g\text{-H} \rightarrow g\text{-HCO}$...	Assumed fast
D3. $g\text{-H}_2\text{CO} + g\text{-HCO} + g\text{-H} \rightarrow g\text{-CH}_2\text{OHCHO}$	3.0×10^{-17}	Conservative estimate, based on methyl formate reaction
E1. $g\text{-CO} + g\text{-H} \rightarrow g\text{-HCO}$...	Assumed fast
E2. $g\text{-HCO} + g\text{-C} \rightarrow g\text{-HC}_2\text{O}$	1.0×10^{-10}	Based on similar gas phase
E3. $g\text{-HC}_2\text{O} + g\text{-H} \rightarrow g\text{-CH}_2\text{CO}$	1.0×10^{-9}	Based on similar gas phase
E4. $g\text{-CH}_2\text{CO} + g\text{-H} \rightarrow g\text{-CH}_2\text{CHO}$	5.0×10^{-9}	Based on similar gas phase
E5. $g\text{-CH}_2\text{CHO} + g\text{-O} \rightarrow g\text{-OCH}_2\text{CHO}$	1.0×10^{-12}	Based on H-atom gas-phase reaction, retarded
E6. $g\text{-OCH}_2\text{CO} + g\text{-H} \rightarrow g\text{-CH}_2\text{OHCHO}$	3.0×10^{-17}	Conservative estimate, based on methyl formate reaction

Note. Reactions A4, B2, D2, and E1 are identical.

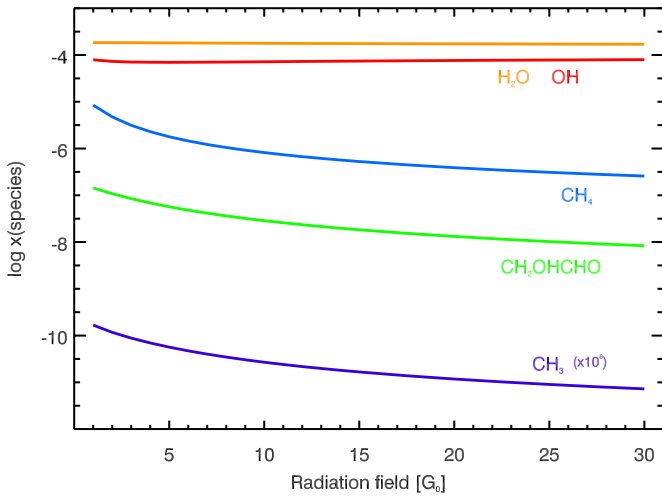


Figure 1. Dependence of glycolaldehyde abundance upon UV radiation field intensity, for mechanism A.

arise from varying the α -parameter in the rate coefficient of the reactions involved in the mechanisms by a factor of up to $10^{\pm 7}$.

4.1. The Effect of Scaling the UV Field Strength on Mechanism A

In order to explore the effects of enhanced UV irradiation of surface ices in mechanism A (Table 1), we have used the standard reaction rates as shown in Table 3, and the more conservative hydrogenation regime (Table 2). We varied the strength of the UV field by up to a factor of 30 over the standard interstellar field, and the results are plotted in Figure 1. Intuitively, one would expect that increased grain

processing of surface-bound H_2O and CH_4 would lead to a greater production of glycolaldehyde. However, higher UV fluxes mean that the gas-phase species which go on to form CH_4 in particular on the grains are destroyed by reaction with abundant photodissociation products like H_3^+ and H^+ . Thus, the limited abundance of grain-surface CH_4 limits the formation of glycolaldehyde. Water ice increases very marginally in abundance when the core is under higher levels of irradiation.

4.2. Reaction Rate Analysis of Mechanism A

Results of the model can be found in Figure 2, where we plot the fractional abundance of glycolaldehyde obtained at the final density of the collapse, n_f , against the scale factor of the “standard” rates, as found in Table 3. We compare models with differing n_f and in the two different hydrogenation regimes, f1 and f2. The fractional abundance of glycolaldehyde in the model is highly dependent on the rate of the final reaction of mechanism A, A5—it scales linearly with the rate until 1–10 times the standard rate, after which the curve turns over to a maximum abundance of $x(\text{CH}_2\text{OHCHO}) \sim 10^{-5}$. The effect of the differing hydrogenation regimes is minimal. The fractional abundance of glycolaldehyde is fairly insensitive to the rates of reactions A1–A3, increasing by only a factor of 10 or so while the rate coefficients span a range of 10^{14} . Reactions A1 and A2 compete with grain-surface hydrogenation of O and C in the provision of OH and CH_3 radicals, respectively. As core density increases, photons become increasingly absorbed, meaning that reaction A3 proceeds with reactants that are products of grain-surface hydrogenation rather than grain-surface photolysis (see, Peeters et al. 2006). Reaction A3 itself is competing with the hydrogenation of adsorbed CO, which dominates at high densities, meaning that the abundance of glycolaldehyde is relatively independent of reactions A1–A3 in general.

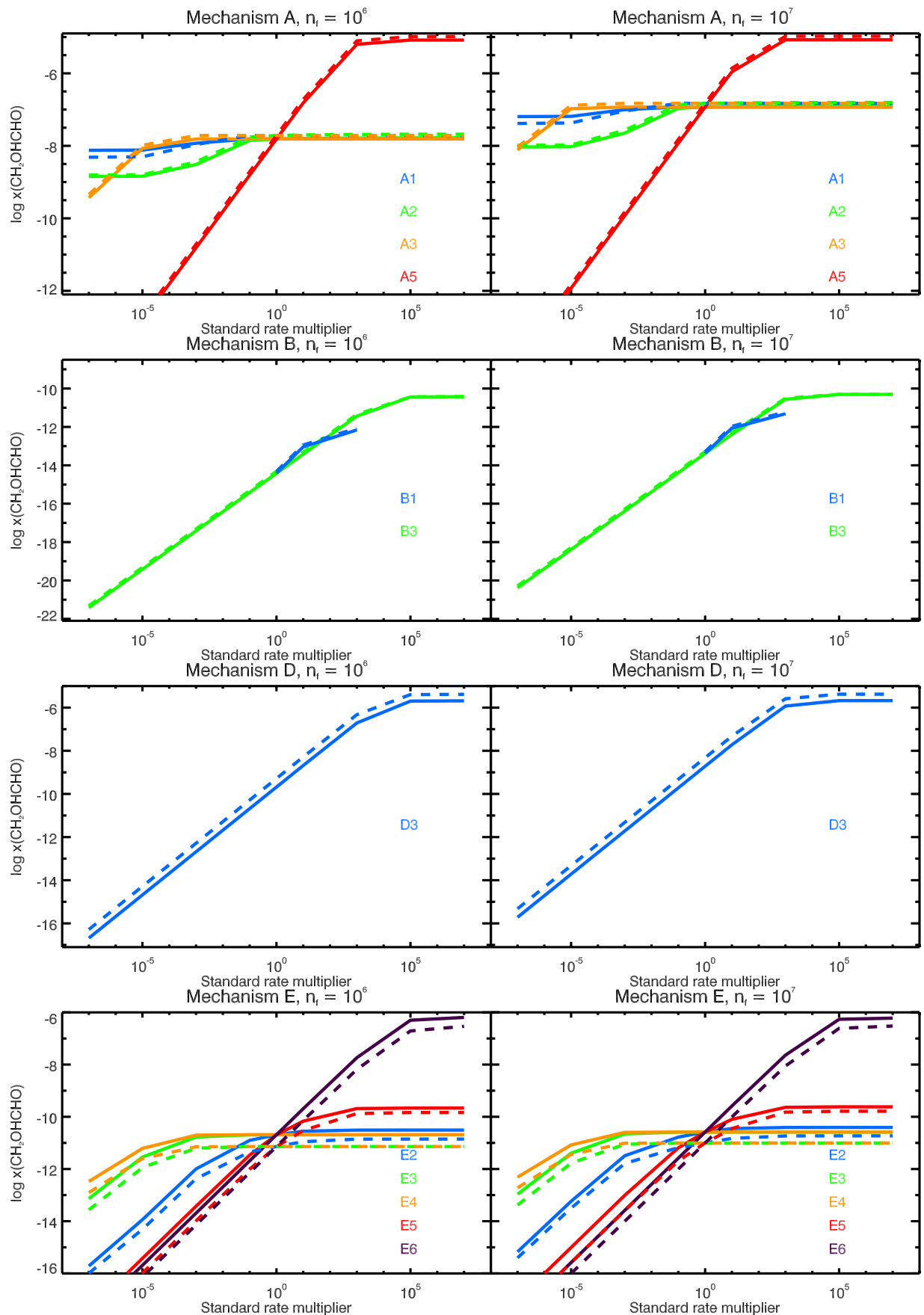


Figure 2. Production of glycolaldehyde via mechanisms A, B, D, and E, for $n_f = 10^6$ and 10^7 cm^{-3} (see Section 4.4 for a description of mechanism C). The solid lines show results using hydrogenation regime f1; the dashed lines, regime f2. Standard rates can be found in Table 3.

(A color version of this figure is available in the online journal.)

Reaction A3 has been studied in the literature, as part of investigations into methanol formation. Experiments on H₂O–CO ice at $T < 20$ K by Hidaka et al. (2004) do not show any evidence of methane production, which implies that abundances of CH₃ are low. It seems likely that methanol production results mainly from the successive hydrogenation of CO (i.e., CO → HCO → H₂CO → CH₃O → CH₃OH) rather than via reaction A3 (Hidaka et al. 2004).

Reaction A4 has also been well studied in the literature (e.g., Hudson & Moore 1999; Watanabe et al. 2003), and is a crucial reaction in many of the mechanisms studied here (it is identical to B2, D2, and E1). HCO ice has not been detected in the interstellar medium, implying that its formation is slower than subsequent reactions, e.g., H + HCO → H₂CO, which have lower activation energies (Watanabe & Kouchi 2002). Indeed, the formation of H₂CO in this way has been shown to be barrierless (Goumans et al. 2007). CO + H has a barrier of several thousand Kelvin in the gas phase (see summary by Hidaka et al. 2007), but barriers on a surface depend on the composition and structure of that surface (Watanabe et al. 2004; Goumans et al. 2008), with, in some cases, the reaction being completely barrierless (Goumans et al. 2008). Hidaka et al. (2007) calculate a rate for A4 from an experiment involving various combinations of CO and H₂O ice. They find that the product k_{HNH} is $\sim 5 \times 10^{-3} \text{ s}^{-1}$, which for 10^{-3} H atoms per square centimeter of surface (n_{H} ; typical for a large grain) gives a reaction timescale on the order of seconds. For small grains, the timescale could be on the order of a year (i.e., fast by astrophysical standards).

Reaction A5 requires the diffusion of molecules and radicals across a grain surface, which is a slow process at 10 K. However, experimental results show that there is some evidence of complex surface reactions, even at 10 K (e.g., Watanabe & Kouchi 2002). Figure 2 suggests that even at rates slower than our conservative standard rate, significant amounts of glycolaldehyde form via this mechanism.

Increasing n_{f} by an order of magnitude from 10^6 to 10^7 cm^{-3} has the effect of increasing glycolaldehyde production for a given reaction rate by a corresponding order of magnitude, approximately. This reflects the greater collisional rate between molecules and grains, and thus a greater freezeout rate. The peak fractional abundance of glycolaldehyde produced via mechanism A, $x(\text{CH}_2\text{OHCHO}) \sim 10^{-5}$, is unaffected by the change in n_{f} , showing that a significant proportion of the available carbon ends up in glycolaldehyde at the most extreme rates investigated, something which is unlikely to occur naturally.

4.3. Reaction Rate Analysis of Mechanism B

The reaction mechanism suggested by Bennett & Kaiser (2007b), which was identified experimentally in the laboratory, is very inefficient at producing glycolaldehyde at 10 K. Even under conditions where the cosmic-ray ionization rate is increased by seven orders of magnitude, less than $x(\text{CH}_2\text{OHCHO}) \sim 10^{-9}$ results (Figure 2). The rates adopted for reactions B1 and B3 are critical to the amount of glycolaldehyde produced, with the yield scaling linearly with the adopted rate. Using our standard rates for B1 and B3, $x(\text{CH}_2\text{OHCHO}) \sim 10^{-13}$ – 10^{-14} , significantly lower than that observed in G31.41+0.31 (Beltrán et al. 2009). Moreover, we do not include the hydrogenation of the hydroxymethyl (CH₂OH) radical to methanol in our reaction scheme, which surely must be rapid and compete with reaction B3.

4.4. Reaction Rate Analysis of Mechanism C

Mechanism C, the only gas-phase reaction mechanism we investigate, is also not particularly efficient in the production of glycolaldehyde, producing $x(\text{CH}_2\text{OHCHO}) \lesssim 10^{-10}$ at the most enhanced values of the reaction rate coefficients. We do not increase the rate coefficient of reaction C1 beyond $6.3 \times 10^{-7} \text{ cm}^3 \text{ s}^{-1}$, since this would be incredibly fast for a gas-phase reaction. In fact, we only vary the rate of C1 for completeness, since the standard reaction rate (from Tanner et al. 1979) is accurate to 25% according to the UfA database. Both reactions C1 and C2 produce linearly increasing amounts of CH₂OHCHO with increasing reaction rate coefficient, producing $x(\text{CH}_2\text{OHCHO}) = 10^{-13}$ at the standard rates. The limiting factor in this mechanism is the availability of gas-phase formaldehyde, which at 10 K is only 1% of the total formaldehyde, the rest being frozen onto grain surfaces. However, we do not include non-thermal desorption mechanisms in our simple model, which could increase the amount of formaldehyde in the gas phase. Roberts et al. (2007) show that non-thermal desorption can return a large proportion of H₂CO to the gas phase in extreme cases. It is not clear how their results would apply to our situation, where the density is larger, and thus freezeout more rapid.

4.5. Reaction Rate Analysis of Mechanism D

This grain-surface reaction based on the work of Beltrán et al. (2009) involves the products of rapid hydrogenation of CO and HCO⁽⁺⁾, meaning that the only instructive reaction rate to investigate is that of reaction D3. We simplify the three-body reaction proposed by Beltrán et al. (2009) with a two-body reaction by assuming that the H-atom addition is rapid. A maximum fractional abundance of glycolaldehyde of $\sim 10^{-6}$ is produced when the standard rate for the reaction is increased by 1000–10,000, depending on n_{f} . At the standard rate, $x(\text{CH}_2\text{OHCHO}) \approx 10^{-9}$ – 10^{-10} , somewhat smaller than derived from their observations, but within their error constraints (see Section 5).

4.6. Reaction Rate Analysis of Mechanism E

The atom-addition mechanism suggested by Charnley & Rodgers (2005) is the most complex that we have considered, involving six two-body reactions. Three of these reactions are reactions with H, which are assumed rapid, but the surface migration of heavier atoms is significantly slower due to the large diffusion barriers involved (e.g., Leitch-Devlin & Williams 1984). The rates of reactions E2–E4 have little effect on the abundance of glycolaldehyde, showing largely flat profiles in Figure 2. The gradient of reaction E5, where an oxygen atom is added to the molecule, is somewhat steeper, but reaction E6 is the crucial reaction in this mechanism. We have assumed a fairly conservative value of $3 \times 10^{-17} \text{ s}^{-1}$ for this reaction, due to a potential barrier in the H-addition process, but if the reaction were 10^3 – 10^5 times faster than expected, then it could produce $x(\text{CH}_2\text{OHCHO}) \sim 10^{-6}$.

4.7. Further Experimentation

The analysis performed thus far has been somewhat artificial, since if the reactions contained in the suggested mechanisms occur, then they likely occur in competition with each other (and other reactions), i.e., reactions in other mechanisms are not “switched off.” To investigate this, we performed two

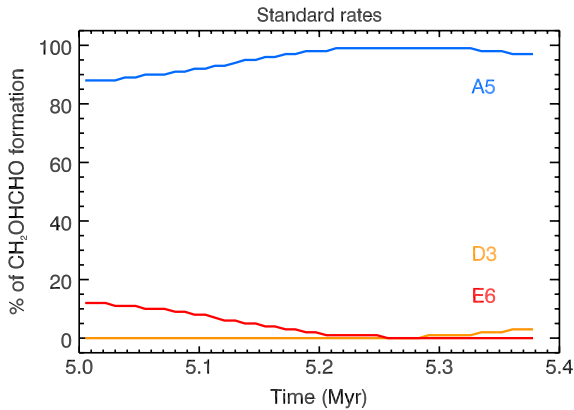


Figure 3. Formation route of glycolaldehyde with all mechanisms in operation, using standard reaction rates.

further experiments where we set the rates of all the reactions considered to their standard rates, and where we set them to “optimal” rates. By optimal here we mean adopting α values for where the rate profiles in Figure 2 turn over to become flat. Rates for mechanism C were kept as standard, since the rate profiles do not turn over.

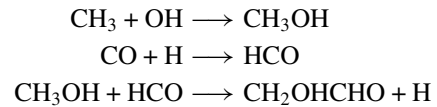
We find that, when using standard rates for all reactions, $x(\text{CH}_2\text{OHCHO}) = 1.5 \times 10^{-7}$. In this competitive environment, reactions A5 and E6 are the dominant routes to the formation of glycolaldehyde, with A5 being the most efficient by a considerable margin as the core collapses (see Figure 3, left). When using “optimal” rates, an extremely large amount of glycolaldehyde can form, $x(\text{CH}_2\text{OHCHO}) = 1.1 \times 10^{-5}$, which is approximately 6% of the elemental carbon abundance of the core. In this case, the most dominant reaction for its formation at later times is B3 (the rate of which has been enhanced 10^5 times); E6 dominates at early times, with a rate enhancement of 10^7 . Given these extreme rate enhancements, this scenario is unlikely.

5. DISCUSSION

Having investigated the formation of glycolaldehyde via five different reaction mechanisms, it is clear that considerable quantities of glycolaldehyde can be produced. Also, very small amounts of glycolaldehyde can result from mechanisms which are inefficient at 10 K (e.g., mechanism B). Many of the rates involved in these mechanisms are completely unknown, and others have a large degree of uncertainty. Given that fractional abundances of glycolaldehyde can vary over 10 orders of magnitude or more in the models, further work needs to be done in order to fully understand how glycolaldehyde forms at low temperatures in dense molecular cores, like those in G31.41+0.31. We are currently undertaking density functional theory calculations for these five mechanisms, with the results to be forthcoming in a future paper.

The fact that glycolaldehyde has been detected in G31.41+0.31 provides us with some constraints on our modeling. Beltrán et al. (2009) estimated that the fractional abundance of glycolaldehyde toward this region was on the order of 10^{-8} . Due to the uncertainties of temperature and column density in their measurements, the errors in this estimate are large: potentially two orders of magnitude (M. Beltrán 2011, private communication). This lower limit of $x(\text{CH}_2\text{OHCHO}) \gtrsim 10^{-10}$ effectively means that we can reasonably exclude mechanisms B and C from further consideration, since they do not produce enough glycolaldehyde even under the most favorable conditions. Mechanism E only produces the required abundances if

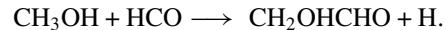
the rate of the final reaction in the scheme is enhanced. Mechanisms A and D have greater fecundity, and Figure 3 shows that mechanism A is considerably more efficient when in competition. Thus, it appears that for the rates we have adopted, the main formation mechanism for glycolaldehyde at 10 K is



on grain surfaces. The formation of both CH_3OH and HCO in ices has been well-studied experimentally (e.g., Watanabe et al. 2003, 2004; Hidaka et al. 2004; Watanabe & Kouchi 2002), and is related, with HCO being a crucial part in the formation of CH_3OH , which is the terminal molecule in the hydrogenation process. Only energetic processes (e.g., UV or cosmic-ray irradiation) will decompose CH_3OH , since H-abstraction to form H_2CO is negligible (Hidaka et al. 2004).

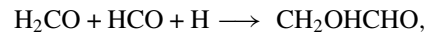
5.1. A Chemical Evaluation of Mechanisms A, D, and E

Building on the astrophysical models, we now consider reactions A, D, and E from a physicochemical perspective, taking account of the intrinsic thermodynamic stability of reagents and products. A full treatment of this is underway, but due to the computationally expensive nature of such an investigation, here we only consider general principles. First, in mechanism A, reaction A5 is found to be particularly efficient at producing glycolaldehyde:



However, A5 is the reaction of a stable molecule (methanol) with a reactive radical (formyl) to give stable glycolaldehyde and an H monoatom. The H monoatom is extremely reactive and even at low temperatures is very mobile, hence the rate of the backward reaction (addition of H to glycolaldehyde) could be expected to be competitive with that of the forward reaction. Preliminary ab initio calculations conducted at the coupled-cluster level with single, double, and triple excitations (CCSD(T)) and a triple-zeta quality basis set shows that, in fact, reaction A5 is endothermic, and consequently the rate of the reaction yielding glycolaldehyde would be very unfavorable.

Reaction D3,



is a three-body reaction which has a vanishingly small probability of occurring, further hindered by the low temperatures considered here. However, the products could be obtained by two sequential two-step reactions: first, reaction of H with HCO yields H_2CO , a barrierless process in the gas phase, according to published theoretical work (Goumans et al. 2007), which could combine with another H_2CO molecule to yield the glycolaldehyde product. However, H_2CO is rather stable and hence the reaction rate for the condensation of two H_2CO molecules could be expected to be rather slow and hence improbable. A second possibility is the reaction of H with H_2CO which according to past work (Woon 2002; Saebo et al. 1983) yields H_3CO as the kinetic product. H_3CO could react with HCO to give glycolaldehyde, and this reaction ought to have a low barrier since both H_3CO and HCO are reactive radical species.

In mechanism E, the final promising path identified from the astrophysical models, glycolaldehyde is assembled from a building block of CO via six stepwise monatomic addition

reactions. Although the constituent reactions of mechanism E are chemically viable, consideration of the physical conditions and the reaction probabilities suggest that this pathway may be an unlikely source of glycolaldehyde. Under the conditions of a temperature of 10 K, only monatomic H is mobile; C and O are static and only become mobile during warm-up, which implies that reactions E2 and E5 are highly unlikely to occur. Hence, these reactions are likely to be rate-limiting. Construction of glycolaldehyde via monatomic addition also depends on a well-defined consecutive set of reactions. In this scheme, HCO reacts with monatomic C (reaction E2), yet monatomic H is present at higher abundance and is known to react without a barrier (Goumans et al. 2007) with HCO, the product of E1, to give H₂CO rather than the product of E2, HC₂O. Since mechanism E is composed of six reactions which are expected to be limited by at least two of those reactions (E2 and E5), we consider this pathway to not be very probable or efficient.

Of the reactions identified by the astrophysical models, it is suggested that mechanism D is the most probable according to chemical considerations. Detailed ab initio calculations are underway to assess the influence of substrates on the reaction barriers and hence quantify the efficiency of mechanisms A, D, and E. It should be noted that mechanisms B and C are viable from a chemical standpoint and these will also be considered in comparison to A, D, and E to assess the most viable scheme.

6. SUMMARY

We have investigated five reaction pathways for the formation of glycolaldehyde, a simple sugar, which have been previously suggested in the astrophysical literature, but not thoroughly tested or justified. By means of a chemical model of an isothermally collapsing molecular core, we have determined that under the physical conditions assumed, mechanisms B and C (suggested by Bennett & Kaiser 2007b; Halfen et al. 2006, respectively) are relatively inefficient and are unlikely to be the major pathways to the formation of glycolaldehyde. Mechanisms D and E (suggested by Beltrán et al. 2009; Charnley & Rodgers 2005, respectively) can reach observed fractional abundances of glycolaldehyde if reaction rates are enhanced by factors of 100 or more over those we have chosen as standard. Finally, mechanism A, from the work of Sorrell (2001), can produce glycolaldehyde very efficiently; however, in the high-density regions around forming protostars, photons are unlikely to penetrate enough to initiate the reaction scheme as it is. Instead, the initial reactants, OH and CH₃, are amply supplied by the freezeout and subsequent hydrogenation of atoms and smaller radicals.

Further evaluation of the reaction schemes taking reagent and product stability into account leads us to expect that mechanism A may not be as efficient as the astrophysical modeling suggests because of a high barrier for the final step in the formation of glycolaldehyde. However, mechanism D may be more likely, provided the final reaction in the scheme proceeds as two two-body reactions involving H₃CO and HCO radicals, rather than a single three-body reaction. Detailed examination of the reaction barriers according to high-level quantum chemical methods is currently being undertaken, taking into account the role of different substrates.

Finally, the list of reactions considered here is not exhaustive and we are seeking to use astrophysical modeling, quantum chemical and experimental approaches to identify whether other, as yet unreported, pathways are more efficient at producing glycolaldehyde.

The authors appreciate fruitful discussions with T. P. M. Goumans, which have benefited the content of this paper. Funding for this work was provided by the Leverhulme Trust to P.M.W. and D.J.B. F.P. acknowledges support from the LASSIE Initial Training Network under the European Community's Seventh Framework Programme FP7/2007-2013 under grant agreement No. 238258.

REFERENCES

- Beltrán, M. T., Codella, C., Viti, S., Neri, R., & Cesaroni, R. 2009, *ApJ*, **690**, L93
- Bennett, C. J., & Kaiser, R. I. 2007a, *ApJ*, **660**, 1289
- Bennett, C. J., & Kaiser, R. I. 2007b, *ApJ*, **661**, 899
- Bergin, E. A., Maret, S., van der Tak, F. F. S., et al. 2006, *ApJ*, **645**, 369
- Breslow, R. 1959, *Tetrahedron Lett.*, 1, 22
- Butlerow, A. 1861, *C. R. Acad. Sci., Paris*, **53**, 145
- Cazaux, S., & Tielens, A. G. G. M. 2004, *ApJ*, **604**, 222
- Charnley, S. B., & Rodgers, S. D. 2005, in *IAU Symp. 231, Astrochemistry: Recent Successes and Current Challenges*, ed. D. C. Lis, G. A. Blake, & E. Herbst (Cambridge: Cambridge Univ. Press), 237
- Collins, P., & Ferrier, R. 1995, *Monosaccharides: Their Chemistry and Their Roles in Natural Products* (New York: Wiley)
- Garrod, R., Park, I. H., Caselli, P., & Herbst, E. 2006, *Faraday Discuss.*, **133**, 51
- Garrod, R. T., Weaver, S. L. W., & Herbst, E. 2008, *ApJ*, **682**, 283
- Goumans, T. P. M., Catlow, C. R. A., & Brown, W. A. 2008, *J. Chem. Phys.*, **128**, 134709
- Goumans, T. P. M., Wander, A., Catlow, C. R. A., & Brown, W. A. 2007, *MNRAS*, **382**, 1829
- Halfen, D. T., Apponi, A. J., Woolf, N., Polt, R., & Ziurys, L. M. 2006, *ApJ*, **639**, 237
- Hidaka, H., Kouchi, A., & Watanabe, N. 2007, *J. Chem. Phys.*, **126**, 204707
- Hidaka, H., Watanabe, N., Shiraki, T., Nagaoka, A., & Kouchi, A. 2004, *ApJ*, **614**, 1124
- Hollis, J. M., Lovas, F. J., & Jewell, P. R. 2000, *ApJ*, **540**, L107
- Hotzel, S., Harju, J., & Juvela, M. 2002, *A&A*, **395**, L5
- Hudson, R. L., & Moore, M. H. 1999, *Icarus*, **140**, 451
- Jalbout, A. F., Abrell, L., Adamowicz, L., et al. 2007, *Astrobiology*, **7**, 433
- Kaiser, R. I. 2002, *Chem. Rev.*, **102**, 1309
- Kaiser, R. I., Eich, G., Gabrysch, A., & Roessler, K. 1997, *ApJ*, **484**, 487
- Laas, J. C., Garrod, R. T., Herbst, E., & Widicus Weaver, S. L. 2011, *ApJ*, **728**, 71
- Lai, S.-P., Velusamy, T., Langer, W. D., & Kuiper, T. B. H. 2003, *AJ*, **126**, 311
- Leitch-Devlin, M. A., & Williams, D. A. 1984, *MNRAS*, **210**, 577
- Molinari, S., Brand, J., Cesaroni, R., & Palla, F. 2000, *A&A*, **355**, 617
- Öberg, K. I., Garrod, R. T., van Dishoeck, E. F., & Linnartz, H. 2009, *A&A*, **504**, 891
- Pagani, L., Bacmann, A., Cabrit, S., & Vastel, C. 2007, *A&A*, **467**, 179
- Peeters, Z., Rodgers, S. D., Charnley, S. B., et al. 2006, *A&A*, **445**, 197
- Remijan, A., Shiao, Y.-S., Friedel, D. N., Meier, D. S., & Snyder, L. E. 2004, *ApJ*, **617**, 384
- Roberts, J. F., Rawlings, J. M. C., Viti, S., & Williams, D. A. 2007, *MNRAS*, **382**, 733
- Saebø, S., Radom, L., & Schaefer, H. F., III. 1983, *J. Chem. Phys.*, **78**, 845
- Snyder, L. E. 2006, *Proc. Natl Acad. Sci.*, **103**, 12243
- Sofia, U. J., & Meyer, D. M. 2001, *ApJ*, **554**, L221
- Sorrell, W. H. 2001, *ApJ*, **555**, L129
- Tanner, S. D., Mackay, G. I., & Bohme, D. K. 1979, *Can. J. Chem.*, **57**, 2350
- Tielens, A. 1989, in *IAU Symp. 135, Interstellar Dust*, ed. L. J. Allamandola & A. G. G. M. Tielens (Dordrecht: Kluwer), 239
- Tielens, A. G. G. M., & Whittet, D. C. B. 1997, in *IAU Symp. 178, Molecules in Astrophysics: Probes & Processes*, ed. E. F. van Dishoeck (Dordrecht: Kluwer), 45
- Viti, S., Caselli, P., Hartquist, T. W., & Williams, D. A. 2001, *A&A*, **370**, 1017
- Viti, S., Collings, M. P., Dever, J. W., McCoustra, M. R. S., & Williams, D. A. 2004, *MNRAS*, **354**, 1141
- Watanabe, N., & Kouchi, A. 2002, *ApJ*, **571**, L173
- Watanabe, N., Nagaoka, A., Shiraki, T., & Kouchi, A. 2004, *ApJ*, **616**, 638
- Watanabe, N., Shiraki, T., & Kouchi, A. 2003, *ApJ*, **588**, L121
- Weber, A. L. 1998, *Orig. Life Evol. Biosph.*, **28**, 259
- Williams, D. A., Brown, W. A., Price, S. D., Rawlings, J. M. C., & Viti, S. 2007, *Astron. Geophys.*, **48**, 1.25
- Woon, D. E. 2002, *ApJ*, **569**, 541